Planta (1997) 201: 84–95

Planta

Parallel control of the inward-rectifier K^+ channel by cytosolic free Ca^{2+} and pH in *Vicia* guard cells

Alexander Grabov, Michael R. Blatt

Laboratory of Plant Physiology and Biophysics, University of London, Wye College Wye, Kent, TN25 5AH, UK

Received: 30 July 1996 / Accepted: 27 August 1996

Abstract. The influence of cytosolic pH (pH_i) in controlling K^+-channel activity and its interaction with cytosolic-free Ca^{2+} concentration ($[Ca^{2+}]_i$) was examined in stomatal guard cells of *Vicia faba* L. Intact guard cells were impaled with multibarrelled microelectrodes and K^+-channel currents were recorded under voltage clamp while pH_i or $[Ca^{2+}]_i$ was monitored concurrently by fluorescence ratio photometry using the fluorescent dyes 2′,7′-bis (2-carboxyethyl)-5(6)-carboxyfluorescein (BCECF) and Fura-2. In 10 mM external K^+ concentration, current through inward-rectifying K^+ channels ($I_{K,in}$) was evoked on stepping the membrane from a holding potential of −100 mV to voltages from −120 to −250 mV. Challenge with 0.3–30 mM Na^+-butyrate and Na^+-acetate outside imposed acid loads, lowering pH_i from a mean resting value of 7.64 ± 0.03 ($n = 25$) to values from 7.5 to 6.7. The effect on pH_i was independent of the weak acid used, and indicated a H^+-buffering capacity which rose from 90 mM H^+/pH unit near 7.5 to 160 mM H^+/pH unit near pH_i 7.0. With acid-going pH_i, $I_{K,in}$ was promoted in scalar fashion, the current increasing in magnitude with the acid load, but without significant effect on the current relaxation kinetics at voltages negative of −150 mV or the voltage-dependence for channel gating. Washout of the weak acid was followed by transient rise in pH_i lasting 3–5 min and was accompanied by a reduction in $I_{K,in}$ before recovery of the initial resting pH_i and current amplitude. The pH_i-sensitivity of the current was consistent with a single, titratable site for H^+ binding with a pK_a near 6.3. Acid pH_i loads also affected current through the outward-rectifying K^+ channels ($I_{K,out}$) in a manner antiparallel to $I_{K,in}$. The effect on $I_{K,out}$ was also scalar, but showed an apparent pK_a of 7.4 and was best accommodated by a cooperative binding of two H^+. Parallel measurements showed that Na^+-butyrate loads were generally without significant effect on $[Ca^{2+}]_i$, except when pH_i was reduced to 7.0 and below. Extreme acid loads evoked reversible increases in $[Ca^{2+}]_i$ in roughly half the cells measured, although the effect was generally delayed with respect to the time course of pH_i changes and K^+-channel responses. The action on $[Ca^{2+}]_i$ coincided with a greater variability in $I_{K,in}$ stimulation evident at pH_i values around 7.0 and below, and with negative displacements in the voltage-dependence of $I_{K,in}$ gating. These results distinguish the actions of pH_i and $[Ca^{2+}]_i$ in modulating $I_{K,in}$; they delimit the effect of pH_i to changes in current amplitude without influence on the voltage-dependence of channel gating; and they support a role for pH_i as a second messenger capable of acting in parallel with, but independent of $[Ca^{2+}]_i$ in controlling the K^+ channels.

Key words: K^+ channel, outward-rectifying – Ca^{2+}/H^+ interaction – Fluorescence ratio photometry – Voltage clamp – Signal transduction – *Vicia* guard-cell plasma membrane

Introduction

It is generally recognised that the K^+ conductance of the guard-cell plasma membrane is dominated by two distinct classes of K^+ channels which differ in their voltage dependencies, agonist and antagonist sensitivities, as well as their gating kinetics (Schroeder 1992; Blatt and Thiel 1993). Of these, the class of inward-rectifying channels comprises an important pathway for K^+ flux at millimolar external K^+ concentrations. Activation of this K^+ current ($I_{K,in}$) is evident on hyperpolarisation both in the intact guard cells and in their protoplasts (Blatt and Thiel 1993). This bias to negative-going membrane voltages favours K^+ flux into

Abbreviations: BCECF = 2′,7′-bis (2-carboxyethyl)-5(6)-carboxy fluorescein; $[Ca^{2+}]_i$ = cytosolic free Ca^{2+} concentration; g_K = ensemble (steady-state) K^+-channel conductance; $I_{K,out}$, $I_{K,in}$ = outward-, inward-rectifying K^+ channel (current); I-V = current-voltage (relation); Mes = 2-(N-morpholinolethanesulfonic acid; pH_i = cytosolic pH; V = membrane potential

Correspondence to: M.R. Blatt; Tel: 44 (1233) 813288; Fax: 44 (1233) 813140; E-mail: mblatt@wye.ac.uk

the cell (Blatt 1992) and, hence, stomatal opening which is realised through a net influx of osmotically active solutes – notably a flux of K^+ across the plasma membrane into the cytoplasm and vacuole – and the consequent rise in guard cell turgor.

Some detail of the intracellular signal cascades controlling these channels is now understood, drawing on studies of hormone action, especially of abscisic acid (ABA) which promotes stomatal closure (MacRobbie 1992; Assmann 1993; Blatt and Thiel 1993). Modulation of both $[Ca^{2+}]_i$ and pH_i have been found to affect K^+ and anion channels at the plasma membrane (Hedrich et al. 1990; McAinsh et al. 1990; Gilroy et al. 1991; Irving et al. 1992; Schroeder and Keller 1992; Blatt and Armstrong 1993; Lemtiri-Chlieh and MacRobbie 1994). The action of cytosolic pH is most pronounced on the outward-rectifying K^+ channels ($I_{K,out}$) (Blatt and Armstrong 1993), which are virtually $[Ca^{2+}]_i$-insensitive. Control of $I_{K,in}$, by contrast, has generally been linked to increases in $[Ca^{2}+]_i$ (Schroeder and Hagiwara 1989; McAinsh et al. 1990), mediated either through Ca^{2+} release from intracellular stores (Blatt et al. 1990; Gilroy et al. 1990; Lemtiri-Chlieh and MacRobbie 1994) or influx across the plasma membrane (Schroeder and Hagiwara 1990; Fairley-Grenot and Assmann 1992). Nonetheless, $I_{K,in}$ – or one of the major signalling elements controlling these channels – is also sensitive to pH_i in a manner antiparallel to that of $I_{K,out}$. Experimentally lowering pH_i through application of weak acids has been shown to activate $I_{K,in}$ (Blatt and Armstrong 1993), and the current is suppressed on exposures to peptide homologues of auxin-binding proteins which raise pH_i (Thiel et al. 1993). Furthermore, control by ABA of $I_{K,in}$ is lost in parallel with that of $I_{K,out}$ in guard cells of transgenic *Nicotiana* carrying a mutant *abi1* gene from *Arabidopsis* (Armstrong et al. 1995). This gene encodes a mutant protein phosphatase (Leung et al. 1994; Meyer et al. 1994) and appears to uncouple the control of $I_{K,out}$ from ABA-evoked changes in pH_i (Armstrong et al. 1995). Thus, circumstantial evidence points to two signalling pathways, associated with $[Ca^{2+}]_i$ and pH_i, that contribute to control of the K^+ channels.

These arguments aside, whether the $[Ca^{2+}]_i$ and pH_i signals can act independently has remained uncertain. On one hand, changes in pH_i, K^+-channel gating (Armstrong et al. 1995) and stomatal aperture (Allan et al. 1994) clearly do occur without measurable changes in $[Ca^{2+}]_i$ and, equally, Ca^{2+}-dependent inactivation of $I_{K,in}$ can proceed even when pH_i is buffered (Blatt and Armstrong 1993; Lemtiri-Chlieh and MacRobbie 1994). On the other hand, it is conceivable that the pH_i signals evoked by hormonal and other stimuli in many circumstances could interact with $[Ca^{2+}]_i$ to modify the gating of $I_{K,in}$. Among others, pH_i is known to affect the binding of inositol-1,4,5-trisphosphate for its receptor that leads to cytoplasmic Ca^{2+} release (Busa 1986; Taylor and Richardson 1991) and, in guard cells, pH_i also affects the gating of vacuolar ion channels that may contribute to $[Ca^{2+}]_i$ changes, either directly or indirectly (Ward and Schroeder 1994; Schulzlessdorf and Hedrich 1995).

In order to place the pH_i sensitivity of K^+-channel gating within a quantitative framework, and to address the issue of pH_i and $[Ca^{2+}]_i$ interaction, we have determined the characteristics of $I_{K,in}$ during challenge with cytoplasmic acid loads while monitoring pHi and $[Ca^{2+}]_i$ by fluorescence ratio photometry. The results show that the K^+ channel is subject to control by pH_i and that the effects of pH_i are experimentally separable from the action of $[Ca^{2+}]_i$ on the channel, although the two ionic messengers do interact. These data are generally consistent with the pattern of ionic second-messenger responses observed during ABA and auxin stimuli, and support a role for pH_i in controlling $I_{K,in}$ independent of $[Ca^{2+}]_i$.

Materials and methods

Plant culture and experimental protocol. Vicia faba L., cv. (Bunyan) Bunyard Exhibition (Unwins Seeds, Histon, Cambs. UK), was grown on washed vermiculite with Hoagland's Salts medium and epidermal strips were prepared as described before from newly expanded leaves taken four to six weeks after sowing (Blatt 1992). Surface areas and volumes of impaled cells were calculated assuming a cylindrical geometry (Blatt, 1992). Epidermal peels were fixed to the glass bottom of the experimental chamber after coating the chamber surface with an optically clear and pressure-sensitive, silicone adhesive (no. 355 medical adhesive; Dow Corning, Brussels, Belgium), and all operations were carried out on a Zeiss Axiovert microscope (Zeiss, Oberkochen, Germany) fitted with Nomarski Differential Interference Contrast optics. Measurements were carried out in rapidly flowing solutions (10 ml/min, ≈ 20 chamber volumes/min). The standard perfusion medium was prepared with 5 mM 2-(N-morpholino)propanesulfonic acid (Mes, pK_a = 6.1) titrated to its pK_a with $Ca(OH)_2$ (final $[Ca^{2+}]$ ≈ 1 mM). Butyrate and acetate for cytoplasmic acid loading were prepared as 1 M stocks by titrating the free acids to pH 6.1 with NaOH; the weak acids were subsequently diluted and KCl included as required. Ambient temperatures were 20–22 °C.

Microelectrodes. Recordings were obtained using four-barrelled microelectrodes coated with paraffin to reduce electrode capacitance (Blatt 1992; Blatt and Armstrong 1993). Current-passing and voltage-recording barrels were filled with 200 mM K^+-acetate (pH 7.5) to minimize salt leakage and salt-loading artifacts associated with the Cl^- anion without imposing a significant acid or alkaline load (Blatt and Armstrong 1993). In some experiments, the electrolytes were first passed over a 1,2-bis(2-aminophenoxy)ethane-N,N,N',N'-tetraacetic acid (BAPTA)-based Ca^{2+}-binding matrix ("Ca^{2+} sponge"; Molecular Probes, Eugene, Ore., USA) to avoid possible $[Ca^{2+}]_i$ loading from the microelectrode. Connection to amplifier headstages were via 1 M KCl Ag-AgCl halfcells, and a matching halfcell and 1 M KCl-agar bridge served as the reference (bath) electrode.

Electrical. Mechanical, electrical and software design have been described previously (see Blatt 1992). Current-voltage (I-V) relations were determined by the two-electrode method with the voltage clamp under microprocessor control using a WyeScience μP amplifier and μLAB analog/digital interface and software (WyeScience, Wye, Kent). Steady-state I-V relations were recorded by clamping cells to a bipolar staircase of command voltages alternating positive and negative from the free-running membrane potential, V_m. For time-dependent characteristics, current and voltage were sampled continuously, nominally at 2 kHz with a low-pass filter cut-off frequency of 1 kHz.

Fluorescence microphotometry. Cytosolic pH and $[Ca^{2+}]_i$ were recorded by fluorescence ratio photometry using a Cairn "spinning-wheel" fluorescence microphotometer (Cairn Research,

Faversham, Kent, UK) and the fluorescent dyes BCECF and Fura-2 (Molecular Probes), respectively. For pH_i measurements, BCECF was excited with light filtered by 440- and 490-nm interference filters (Schott, Mainz, Germany; 10 nm half-bandwidths) and dye fluorescence was recorded after filtering through a 535-nm interference filter (Schott). The ratio of Fura-2 fluorescence after excitation at 340 and 380 nm (Schott filters) was used to determine $[Ca^{2+}]_i$. Fluorescence was sampled at 64 Hz/wavelength in each case, samples being averaged over 1-s intervals and analysed in real time using Cairn Research fluorescence software. All fluorescence signals were adjusted to give zero background prior to dye injections. Dye loading was by iontophoresis (below), and was judged successful by dye distribution restricted to the cytoplasm and by stabilisation of the fluorescence ratios. Calibrations for pH_i were carried out in vitro in 100 mM KCl, 1 mM $MgCl_2$, and 10 mM NaCl with 10 mM Mes/Hepes buffer (pH 7.5); in-vivo calibrations were carried out against 50 mM K^+-Mes (pH 6.1), K^+-Mops (pH 7.2) and K^+-Caps (pH 8.0) buffers after permeabilising with 5 $\mu g \cdot ml^{-1}$ gramicidin. Calibrations for $[Ca^{2+}]_i$ were carried out similarly, after buffering $[Ca^{2+}]$ with EGTA (Bush and Jones 1990; Fricker et al. 1991; McCormack and Cobbold 1991) in vitro. In-vivo calibrations were carried out after permeabilising with 5 $\mu g \cdot ml^{-1}$ nystatin, with 10 $\mu g \cdot ml^{-1}$ ionomycin or with 10 $\mu g \cdot ml^{-1}$ A23187Br (Molecular Probes) and yielded comparable minima for the fluorescence ratio on $[Ca^{2+}]_i$ depletion. Correction of Fura-2 fluorescence for the pH-dependence of the dye indicated that the estimates of $[Ca^{2+}]_i$ might be underestimated by 20–25% in 30 mM Na^+-butyrate (Morris et al. 1994). Otherwise, the results were not significantly altered and the data are therefore presented without correction.

Iontophoresis. Loading of guard cells with the fluorescent dyes was achieved by iontophoresis using a WyeScience iontophoresis module connected to two barrels of the four-barrelled microelectrodes employed for electrical recording. For dye loading, one barrel was generally filled with 200 mM K^+-acetate (pH 7.5) and the second barrel contained 0.1 mM BCECF or Fura-2. Injection currents were typically 2–5 nA over 5–8 min and resulted in cytosolic dye concentrations of 50–100 μM. Dye concentrations were estimated from the fluorescent yields at 440 nm for BCECF, at 380 nm and from fluorescence quenching in the presence of nystatin and Mn^{2+} for Fura-2 (McCormack and Cobbold 1991), and were compared with dye loads estimated from the iontophoresis currents (Purves 1981).

Numerical analyses and calculation of H^+ buffer capacity. Data analysis was carried out by non-linear, least-squares (Marquardt 1963) and, where appropriate, results are reported as the mean ± standard error of (n) observations.

The pH_i sensitivities of $I_{K,in}$ and $I_{K,out}$ were determined by fittings (Marquardt 1963) to a Hill titration function (Segel 1993), for $I_{K,in}$ of the form

$$g_{K,max} = \frac{g_{K,pHmax}[H^+]^n}{K_d^n + [H^+]^n} \quad \text{(Eq.1a)}$$

and for $I_{K,out}$ of the form

$$g_{K,max} = \frac{g_{K,pHmax}K_d^n}{K_d^n + [H^+]^n} \quad \text{(Eq.1b)}$$

Here $g_{K,max}$ and $g_{K,pH\text{-}max}$ are the conductance maxima at each pH_i and at saturating pH_i, respectively; K_d is the apparent dissociation constant [= alog(-pK_a)]; n is the Hill coefficient and corresponds to the apparent number of H^+ binding per channel.

Cytoplasmic H^+ buffer capacity, β, was determined as derivative

$$\beta = (-)\delta[A^-]_i/\delta pH_i \quad \text{(Eq.2)}$$

where $[A^-]_i$ is the change in concentration of the acid anion in the cytoplasm on adding the weak acid to the bath. The calculation requires only that values for pH_i, pH_o, the pK_as for each weak acid (=4.78 for acetate, 4.82 for butyrate) and the concentration of weak acid added outside are known. It was assumed that the initial concentration of the acid anion was zero in the cytoplasm and $[HA]_i = [HA]_o$ on adding the weak acid. Then, from the Henderson-Hasselbalch equation,

$$[A^-]_i = \frac{[A_{tot}]}{10^{pK_a - pH_i} + 10^{pH_o - pH_i}} \quad \text{(Eq.3)}$$

where pH_i is the final cytoplasmic pH, and $[A_{tot}]$ is the total weak acid added (= $[HA]_o$+ $[A^-]_o$).

Chemicals and solutions. The pH buffers and salts were from Sigma Chemical Co. (St. Louis, Mo., USA). The fluorescent dyes BCECF, Fura-2, the Ca^{2+} buffer BAPTA and "Ca^{2+} sponge" were from Molecular Probes. Otherwise, all chemicals were Analytical Grade from BDH Ltd. (Poole, Dorset, UK).

Results

Acidifying pH_i reversibly activates $I_{K,in}$ and inactivates $I_{K,out}$. To relate pH_i to K^+-channel activities directly, it was our intention to combine voltage-clamp recordings with concurrent measurements of pH_i on a cell-by-cell basis. Because of the difficulty of achieving multiple impalements in cells the size of guard cells, single impalements were made with four-barrelled microelectrodes with two barrels linked to the iontophoresis circuit for dye loading and the remaining barrels used for monitoring the membrane voltage and for passing current during voltage-clamp recording. Fluorescence from dye in the microelectrode was masked from detection by the photometer with the slit diaphragm and, once loaded, guard cells were challenged with weak acid while concurrently recording pH_i and membrane current under voltage clamp.

Data from one experiment (one cell) are summarised in Fig. 1, with the fluorescence signals depicting the time course of the experiment in the lower panel. The fluorescence record was initiated immediately after impalement. Until dye injection was begun 6 min later, no signal was measurable above background at either wavelength (not shown), indicating that dye leakage was insignificant in the absence of injection current and autofluorescence did not contribute to the measurements at these wavelengths. Iontophoretic injection during the subsequent 6.5 min of the recording (diagonal-hatched bar, below) was accompanied by a rise in the fluorescence signals excited at both wavelengths (f_{440} and f_{490}). Once dye fluorescence rose above background, the fluorescence ratio $R_{490/440}$(= f_{490}/f_{440}), which was used to monitor pH_i, stabilised rapidly at a value corresponding to a pH_i near 7.6 (axis, right). Both fluorescence signals began a gradual and roughly exponential decay when the injection current was switched off, but the fluorescence ratio remained stable. Adding Na^+-butyrate to the bath in increasing concentrations at this point resulted in sequential decreases in $R_{490/440}$ corresponding to parallel stepwise decreases in pH_i. Washing the weak acid from the bath thereafter was accompanied by a prominent overshoot in the ratio before it relaxed to a value near the initial pH_i.

The alkaline overshoot is characteristic of recovery from acid loads in guard cells (Blatt and Armstrong

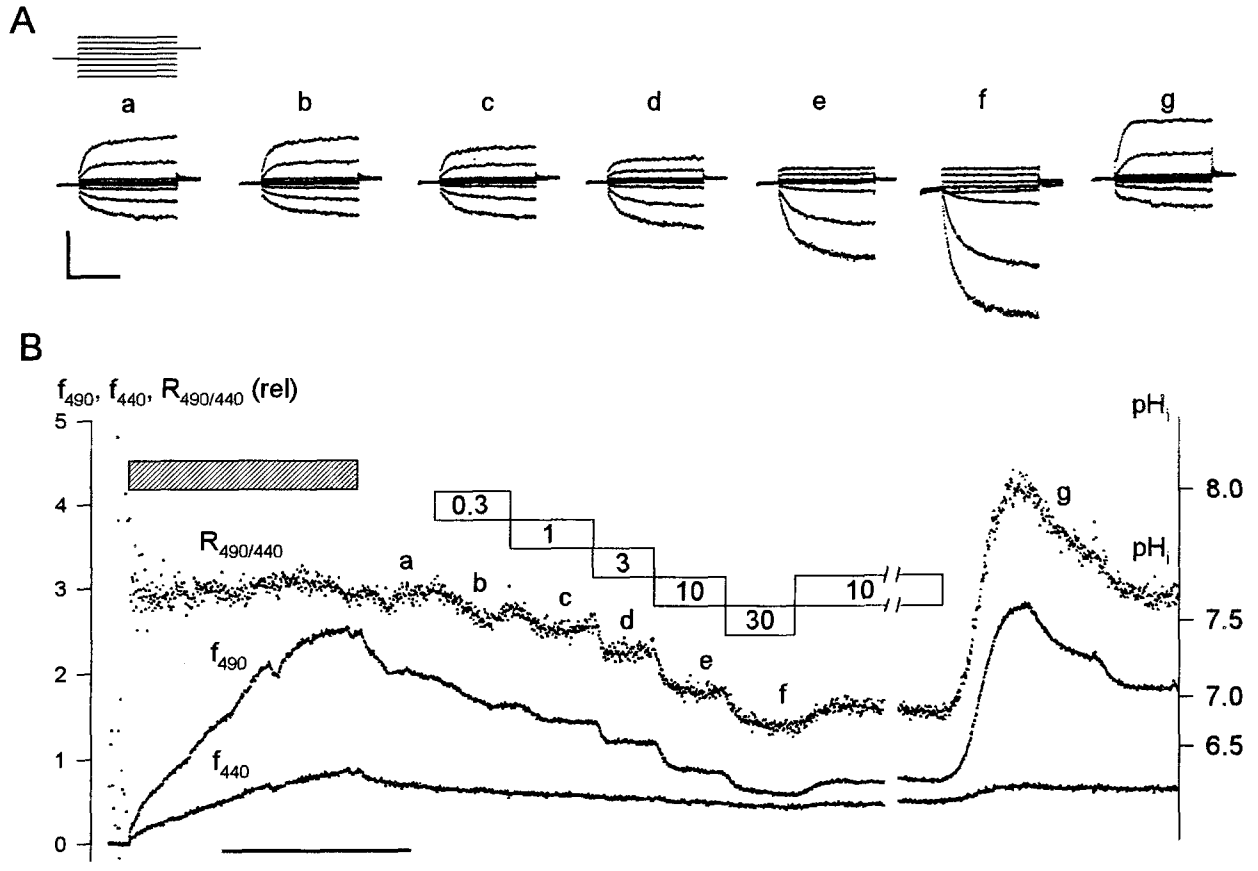

Fig. 1A,B. Acid and alkaline pH_i loads alter inward- ($I_{K,in}$) and outward-rectifying ($I_{K,out}$) K^+-channel activities concurrently. Data from one *Vicia* guard cell bathed in 5 mM Ca^{2+}-Mes, (pH 6.1) with 10 mM KCl and with additions of 0.3, 1, 3, 10 and 30 mM Na^+-butyrate. Cell parameters: surface area, $3.4 \cdot 10^{-5}$ cm^2; volume, 4.6 pl; aperture, 8 μm. **A** Voltage-clamp cycles (*top left*) and current traces recorded at times cross-referenced to the pH_i record in **B** by letter (*a,b,c,...g*). Voltage cycles (8): conditioning voltage, −100 mV; test voltages, +50 to −240 mV; tailing voltage, −30 mV. Scale: vertical, 300 mV or 50 μA cm^{-2}; horizontal, 1 s. **B** Time course of experiment with BCECF fluorescence recordings (*left scale*) with excitation at 440 (f_{440}) and 490 nm (f_{490}) and their ratio ($R_{490/440}$, with pH_i calibration, *right*). Time scale (*below*), 5 min. Time bars (*above*) indicate periods of BCECF injection and of exposures to 0.3–30 mM Na^+-butyrate. Letters (*a,b,c,...g*) indicate times of voltage-clamp scans above

1993; Thiel et al. 1993), and generally is associated with dynamic H^+ buffering that depends on metabolism as well as pH_i (Boron 1977). Similar data were obtained in an additional 24 independent experiments, including those in which Na^+-acetate was substituted for Na^+-butyrate as the weak acid (below), and when the microelectrode was withdrawn from the guard cell after BCECF injection (not shown). By contrast, adding equivalent concentrations of Na^+ as NaCl outside had no measurable effect on pH_i [not shown; see also Blatt and Armstrong (1993), and Blatt (1992) for Na^+-insensitivity of the K^+ channels]. These results argue against any significant interference from dye in the microelectrode, electrolyte leakage or the choice of weak acid.[1] Pooling measurements from all guard cells in these experiments gave a mean pH_i of 7.64 ± 0.03 (n = 25), very close to the values reported from intracellular H^+-sensitive microelectrode (Blatt and Armstrong 1993) and confocal imaging measurements (Thiel et al. 1993).

Measurements with the weak acids permitted an analysis of cytoplasmic H^+ buffering and its dependence on pH_i. The H^+ buffer capacity, β, describes the ability of the cell to accommodate H^+/OH^- loads both through static (ion exchange) and dynamic (metabolic or homeostatic) buffering. An estimate for β can be obtained using weak acids, provided that the weak acid is not itself metabolised significantly during the measurements, because the undissociated acid freely permeates the plasma membrane before equilibrating with the pH of the cytosol (Roos and Boron 1981). Voltage-clamp measurements (see below) also showed no measurable increase in background conductance, so

[1]Diffusion of dye and electrolyte from the microelectrode were unlikely to influence ionic (pH_i and $[Ca^{2+}]_i$) buffering within the cell, as could be estimated from the rate of diffusional dye loading, using measured rates of solute leakage from microelectrodes with similar input resistances (Blatt and Slayman 1983). For the dye, diffusion alone would account at most for about 0.05 $\mu M \cdot min^{-1}$ entering the cytoplasm, assuming a cytoplasmic volume of 1 pl and a leakage rate (adjusted for the 0.1 mM dye concentration in the microelectrode) of up to 0.001 $amol \cdot s^{-1}$. Likewise, estimates for electrolyte leakage (Blatt and Armstrong 1993) anticipate an alkaline pH_i load of approximately 0.01 $mM \cdot min^{-1}$. In practice, these figures are probably significant overestimates when depletion from the microelectrode tip is taken into account (Purves 1981).

providing a check against significant leakage of the acid anion.

Figure 2 summarises the effect on pH_i of acid loads imposed in all experiments with Na^+-butyrate, including data from Fig. 1. Also shown are the results of measurements using Na^+-acetate in place of Na^+-butyrate. In each case the H^+ load was calculated from the measured change in pH_i and the pK_a of the weak acid using Eq. 3 (see *Materials and methods*). Increasing the H^+ load on the cells resulted in a progressive, but non-linear acidification of pH_i, indicating a pronounced pH_i-dependence of β. The solid curve was the best fit to the Henderson-Hasselbalch equation (see *Materials and methods*) and yielded a total cytoplasmic buffer concentration of 275 ± 18 mM with an apparent pK_a of 6.9 ± 0.1. The slope of this curve yields the H^+ buffer capacity as a function of pH_i (*inset*), and pointed to roughly a 1.8-fold increase in β between the resting pH_i of the cells [β ≈ 90 mM H^+/(pH unit)] and pH_i 6.7 [β ≈160 mM H^+/(pH unit)]. Note that the calculations of H^+ loading yielded virtually identical results with both weak acids, again supporting a common and simple action through the imposed H^+ load rather than a secondary response to the acid anion or its metabolism.

Also shown in Fig. 1 in the frame above, are membrane currents recorded under voltage clamp at times throughout the experiment. Clamping the membrane from a conditioning voltage of −100 mV to values between −240 and +50 mV, and thereafter to a tailing voltage of −30 mV uncovered the characteristic time- and voltage-dependent activation of the two K^+-channel currents and their subsequent deactivation (Blatt 1992; Blatt and Armstrong 1993). In these measurements with 10 mM KCl in the bath, $I_{K,out}$ was identified by the time-dependent outward (positive) current recorded on stepping to +8 mV and +50 mV, while $I_{K,in}$ was defined by the time-dependent inward (negative) current recorded at voltages between −140 and −240 mV. Clamp steps at intermediate voltages which activated neither $I_{K,in}$ nor $I_{K,out}$ gave only an instantaneous, time-independent background current (Blatt 1992).

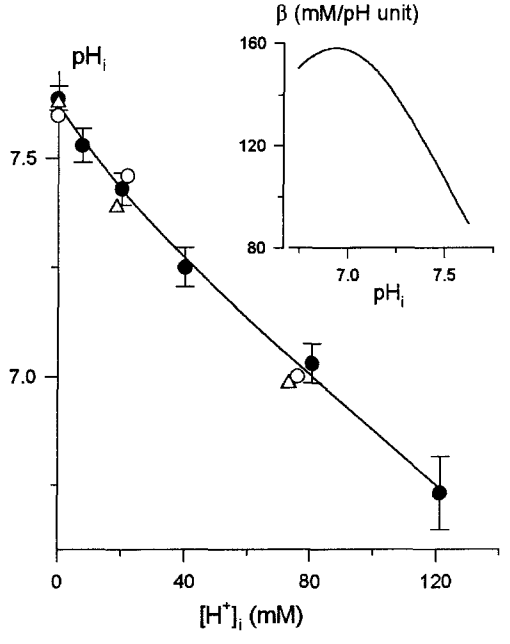

Fig. 2. Weak acids Na^+-butyrate and Na^+-acetate are equally effective in acidifying pH_i. Cytosolic pH (pH_i) determined from BCECF fluorescence ratio recordings in 25 *Vicia* guard cells with Na^+-butyrate (●) and with Na^+-acetate (○, △) as a function of the $[H^+]_i$ load calculated from Eq. 4. Points are means ± SE at each weak acid concentration. *Inset*: H^+ buffer capacity (β) as a function of pH_i

Evident from Fig. 1, the two K^+ currents showed opposing responses to acid loads. Cytosolic acidification, resulted in a sequential reduction of $I_{K,out}$ which decreased approx. 22% in 1 mM butyrate and, in 10 and 30 mM butyrate ($pH_i \leq 7.0$), was fully inactivated (Fig. 1A, center). By contrast, the same acid loads evoked a sequential increase in $I_{K,in}$ which was evident with exposure to as little as 1 mM butyrate ($pH_i \approx 7.4$; compare time-dependent current magnitudes at −240 mV). The effect of pH_i in each case was mediated through the two K^+ channels, as could be demonstrated by $[K^+]_o$ depletion (for $I_{K,in}$) and tail-current analyses (not shown); both currents responded fully within the time-scale of each pH_i change imposed; and recovery parallelled that of pH_i when Na^+-butyrate was washed from the bath (not shown). Indeed, during butyrate washout and the accompanying alkaline pH_i overshoot, both current responses were reversed (Fig. 1A, right): $I_{K,out}$ was enhanced about 30% while $I_{K,in}$ was reduced 25% relative to the control. Again, equivalent results were obtained in all experiments with Na^+-butyrate and when Na^+-acetate was substituted for Na^+-butyrate as the weak acid. Table 1 summarises the mean conductances pooled for $I_{K,in}$ and $I_{K,out}$ relative to the respective controls.

Cytosolic pH controls steady-state K^+-channel current independent of membrane voltage. Analyses of voltage-clamp data indicated that the action of pH_i on both $I_{K,out}$ and $I_{K,in}$ was essentially voltage independent. The steady-state current-voltage (I-V) plots in Fig. 3 were obtained from the data in Fig. 1 after subtracting background ("instantaneous") currents determined in the first 5 ms of each test voltage-clamp step (see Fig. 1). To quantify the voltage-dependence of current activa-

Table 1. The pH_i dependence of inward- and outward-rectifying K^+ channel currents from *Vicia* guard cells. Data from 10 cells with full exposure to 0.3–30 mM Na^+-butyrate, as means ± SE. Relative conductance (g_K/g_K^o) calculated on a cell-by-cell basis at 3 and 30 mM Na^+-butyrate relative to the control with the mean pH_i under acid load indicated in parantheses. Apparent pK_a, Hill coefficient (n) and conductance maximum ($g_{K,max}$) determined by fitting to Eq. 2

Parameter	$I_{K,in}$	$I_{K,out}$
g_K/g_K^o (7.25)	1.47 ± 0.11	0.41 ± 0.11
g_K/g_K^o (6.74)	2.97 ± 0.77	0.022 ± 0.003
pK_a	6.3 ± 0.2	7.4 ± 0.1
n	0.7 ± 0.2	2.4 ± 0.2
$g_{K,max}$ (mS · cm−2)	3.2 ± 0.2	0.8 ± 0.3

tion, each set of curves ($I_{K,in}$ and $I_{K,out}$) was fitted to a Boltzmann function as

$$g_K = \frac{g_{K,max}}{1 + e^{\delta F(V-V_{1/2})/RT}} \quad \text{(Eq.4)}$$

Here the conductance $g_K = I_K(V-E_K)$, its maximum is defined by $g_{K,max}$, δ is the voltage-sensitivity coefficient and corresponds to the apparent gating charge moved within the membrane electric field during channel activation, and F, R and T have their usual meaning. Half-maximal activation ($g_K = 0.5.g_{K,max}$) occurs when the membrane voltage, V, equals $V_{1/2}$ and this value provides a index to the voltage-dependence of gating.

For each of the currents, $I_{K,in}$ and $I_{K,out}$, the curves in Fig. 3 were fitted jointly. Best results were obtained with common values for δ of 1.68 and 2.06 for $I_{K,in}$ and $I_{K,out}$, respectively, consistent with previous analyses (Blatt 1992; Blatt and Armstrong 1993). Joint fittings also gave a common value for $V_{1/2}$ of 4 mV for $I_{K,out}$ (Fig. 3A, inset). For $I_{K,in}$, the fittings likewise indicated little sensitivity of $V_{1/2}$ to the H^+ load, except at the pH_i extremes. Statistically equivalent and, as shown in Fig. 3B, visually satisfactory results were obtained in joint analyses with a common $V_{1/2}$ of −179 mV as when $V_{1/2}$ was allowed to vary between pH_i values. Only in 30 mM Na^+-butyrate did the analysis give significantly better results when $V_{1/2}$ was not held in common and yielded a value of −163 mV. Figure 4 summarises these results for all experiments, including the data from pH_i loads with Na^+-acetate, and shows an appreciable variation for $I_{K,in}$ only at the pH_i extremes, suggesting that pH_i may interact with another factor that affects channel gating under these conditions.

A similar conclusion was drawn from the activation kinetics for $I_{K,in}$. The halftimes ($t_{1/2}$) for current relaxations plotted against pH_i in Fig. 5 were pooled from all joint measurements at −240 mV spanning 3, 10 and 30 mM Na^+-butyrate. As is evident, current relaxations were largely pH_i independent and close to the mean of 134 ms in the control. However, near and below pH_i 7.0, $I_{K,in}$ activation showed greater variance. The means were displaced to longer halftimes, although

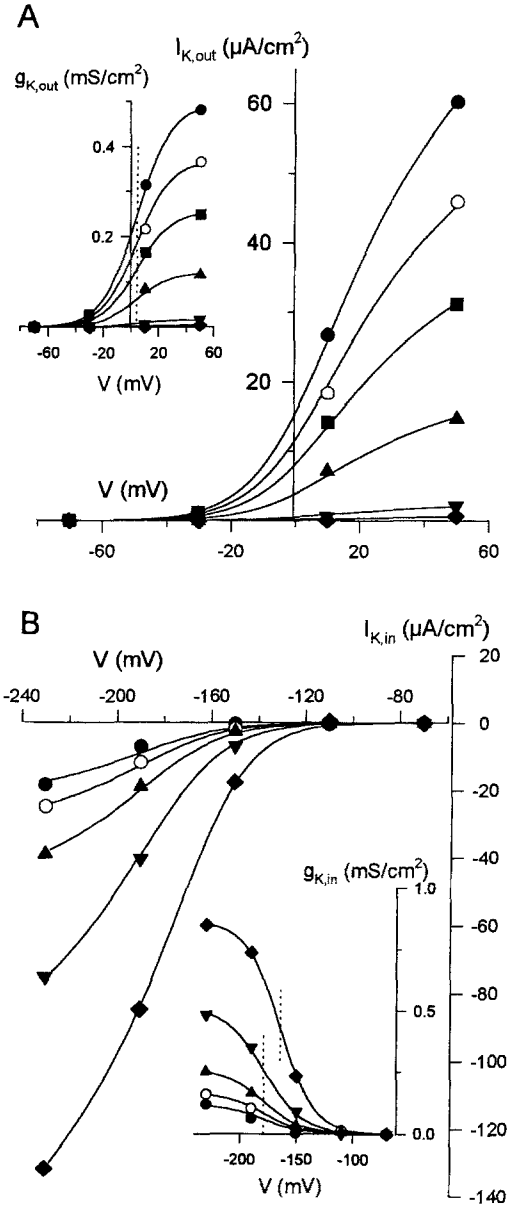

Fig. 3A,B. Inward- ($I_{K,in}$) and outward-rectifying ($I_{K,out}$) K^+-channel currents respond in scalar but opposing fashion to changes in pH_i. Steady-state current-voltage (I-V) curves for $I_{K,out}$ (**A**) and $I_{K,in}$ (**B**) and calculated conductance- (g_K) voltage relations (*insets*) from the current traces in Fig. 1 [symbol, pH_i (*trace reference*): ○, 7.65 (*a*); ■, 7.51 (*c*); ▲, 7.43 (*d*); ▼, 7.10 (*e*); ◆, 6.78 (*f*); ●, 7.92 (*g*)]. Curves are results of joint fittings to the Boltzmann function (Eq. 4) and yielded a common δ each for $I_{K,in}$ and $I_{K,out}$ of 1.68 and 2.06, respectively. A common voltage ($V_{1/2}$) yielding half-maximal conductance was found for $I_{K,out}$ at 4 mV. For $I_{K,in}$ best fittings gave a common $V_{1/2}$ of −179 mV for all but the most acid pH_i (◆), which gave a value of −163 mV. Values for $V_{1/2}$ indicated by *dashed lines* (*insets*)

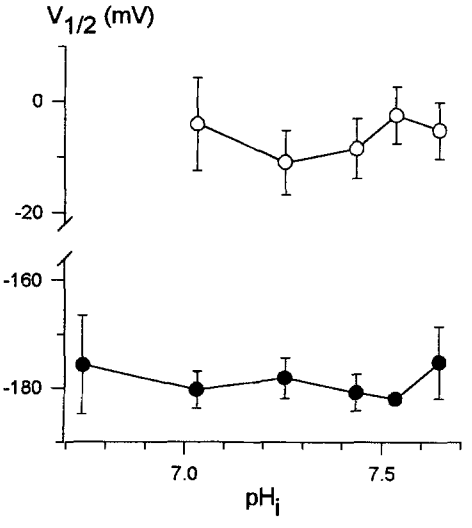

Fig. 4. Voltage-dependence of K^+-channel gating is largely pH_i insensitive. Data pooled from ten *Vicia* guard cells (see also Table 1) challenged with Na^+-butyrate and Na^+-acetate for $I_{K,in}$ (●) and $I_{K,out}$ (○). Voltages ($V_{1/2}$) yielding half-maximal conductance ($g_K = 0.5g_{K,max}$) were found by fitting to Eq. 1 and are plotted as means ± SE against the mean pH_i of acid loads. Note the greater SE at pH_i 6.74 for $I_{K,in}$. Increased SE for $I_{K,out}$ is a consequence of the much reduced current signal at acid pH_i

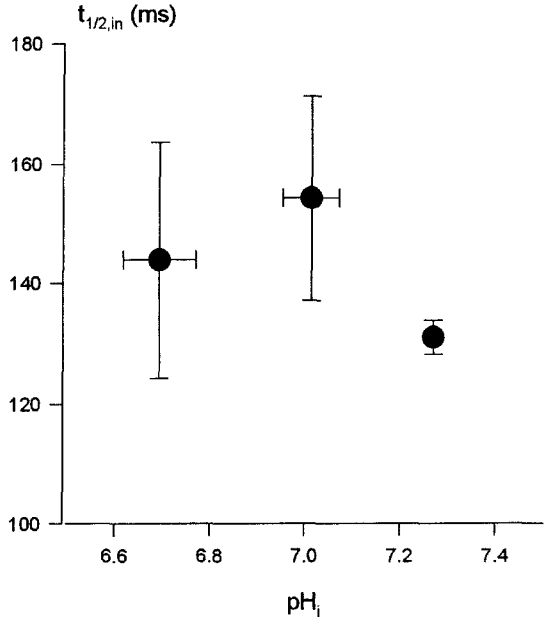

Fig. 5. Halftimes ($t_{1/2}$) for relaxation of the inward-rectifying K^+channel current ($I_{K,in}$) show appreciable variation at the acid pH_i extreme. Data from six *Vicia* guard cells with contiguous measurements in 3, 10 and 30 mM Na^+-butyrate plotted against pH_i. Halftimes determined directly from current traces in each case. Mean halftimes in the absence of Na^+-butyrate, 134 ± 9 ms

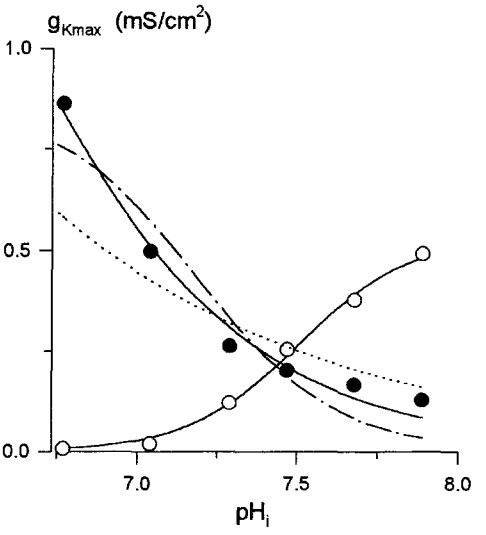

Fig. 6. Titration of conductance maxima ($g_{K,max}$) for the inward-($I_{K,in}$, ●) and outward-rectifying ($I_{K,out}$, ○) K^+ channels indicates cooperativity of H^+ action on $I_{K,out}$ but not on $I_{K,in}$. Conductance maxima from Fig. 3 and additional fittings for $I_{K,in}$ and $I_{K,out}$ from Fig. 1. The *solid curves* are results of fitting to Eq. 3. Fitted parameters ($I_{K,in}$): Hill coefficient, 0.95; pK_a, 6.4; g_{Kmax}, 3.1 mS·cm^{-2}; ($I_{K,out}$): Hill coefficient, 2.4; pK_a, 7.5; $g_{K,max}$, 0.54 mS·cm^{-2}. Also shown for comparison are best fittings for $I_{K,in}$ with the Hill coefficient n fixed to values of 0.5 (*dotted curve*) and 2 (*dot-dashed curve*)

the difference was not very significant. Because altering channel gating kinetics can be expected to affect macroscopic current relaxations, these data suggest that pH_i acts on the number of channels available or the single-channel conductance (see *Discussion*) but also implied an additional affect on channel gating at the acid pH_i extreme.

As evident from Fig. 1, the principal effect of pH_i was on the magnitude of the two currents. To quantify the pH_i sensitivities of $I_{K,in}$ and $I_{K,out}$, the conductance maxima determined from Eq. 4 were fitted by statistical minimisation (Marquardt 1963) to a Hill titration function (Eq. 1; see *Materials and methods*) to determine the apparent pK_a and number of H^+ ions required for current activation in each case. Conductance maxima and the predicted titration curves for $I_{K,in}$ and $I_{K,out}$ from Fig. 3 are plotted in Fig. 6. Also shown for comparison are the outcomes of analyses with the Hill coefficient n fixed to values of 0.5 and 2 (dotted curves). The results indicated a Hill coefficient of 0.95 and pK_a of 6.4 for $I_{K,in}$, and thus point to the titration of a single H^+-binding site leading to activation of the current. A similar analysis for $I_{K,out}$ yielded a Hill coefficient near 2 and apparent an pK_a of 7.5, roughly consistent with previous estimates (Blatt and Armstrong 1993). Table 1 summarises the results from analyses of all ten experiments entailing measurements over this full range of pH_i values. Overall, the means of the parameters for $I_{K,in}$ were somewhat lower than the estimates obtained in Fig. 6, although the differences were not very significant. However, the wide variance between cells observed at the acid pH_i extreme ($g_{K,max}$ stimulation approx. 300 ± 77% about pH_i 6.7 compared with 47 ± 11% near pH_i 7.3; see Table 1), again suggested that another factor that affected channel gating under these conditions, and lead us to investigate the interaction of acid pH_i with $[Ca^{2+}]_i$.

Cytosolic pH- and $[Ca^{2+}]_i$-mediated controls of $I_{K,in}$ are distinct. The action of pH_i, especially in activating $I_{K,in}$, appeared to militate against explanations invoking a $[Ca^{2+}]_i$ intermediate. Unlike the effects of $[Ca^{2+}]_i$ on the current, pH_i affected the magnitude of $I_{K,in}$ in an essentially scalar (voltage-independent) fashion and without altering the current relaxation kinetics, except at the acid pH_i extreme (compare Blatt and Armstrong 1993; Schroeder and Hagiwara 1989). However, neither these data in isolation – nor single-channel studies – rule out an interaction between pH_i and $[Ca^{2+}]_i$ per se, nor additive effects of $[Ca^{2+}]_i$ on the current. Indeed, the higher variability of $I_{K,in}$ observed under extreme acid pH_i loads might be understood in terms of an additional and concurrent modulation by $[Ca^{2+}]_i$ or of competition between H^+ and Ca^{2+} for a common binding site.

To assess the possible interaction of pH_i with $[Ca^{2+}]_i$, distinct from their coordinate actions on $I_{K,in}$ activity, experiments were carried out to record $[Ca^{2+}]_i$ and its response to cytoplasmic H^+ loads. In this case, guard cells were injected with the Ca^{2+}-sensitive, fluorescent dye Fura-2, after impalement with four-barrelled microelectrodes, the cells were challenged with 1–30 mM Na^+-butyrate and membrane current recorded under voltage clamp as before. Fura-2 fluorescence was monitored at 520 nm after excitation with 340-nm and 380-nm light

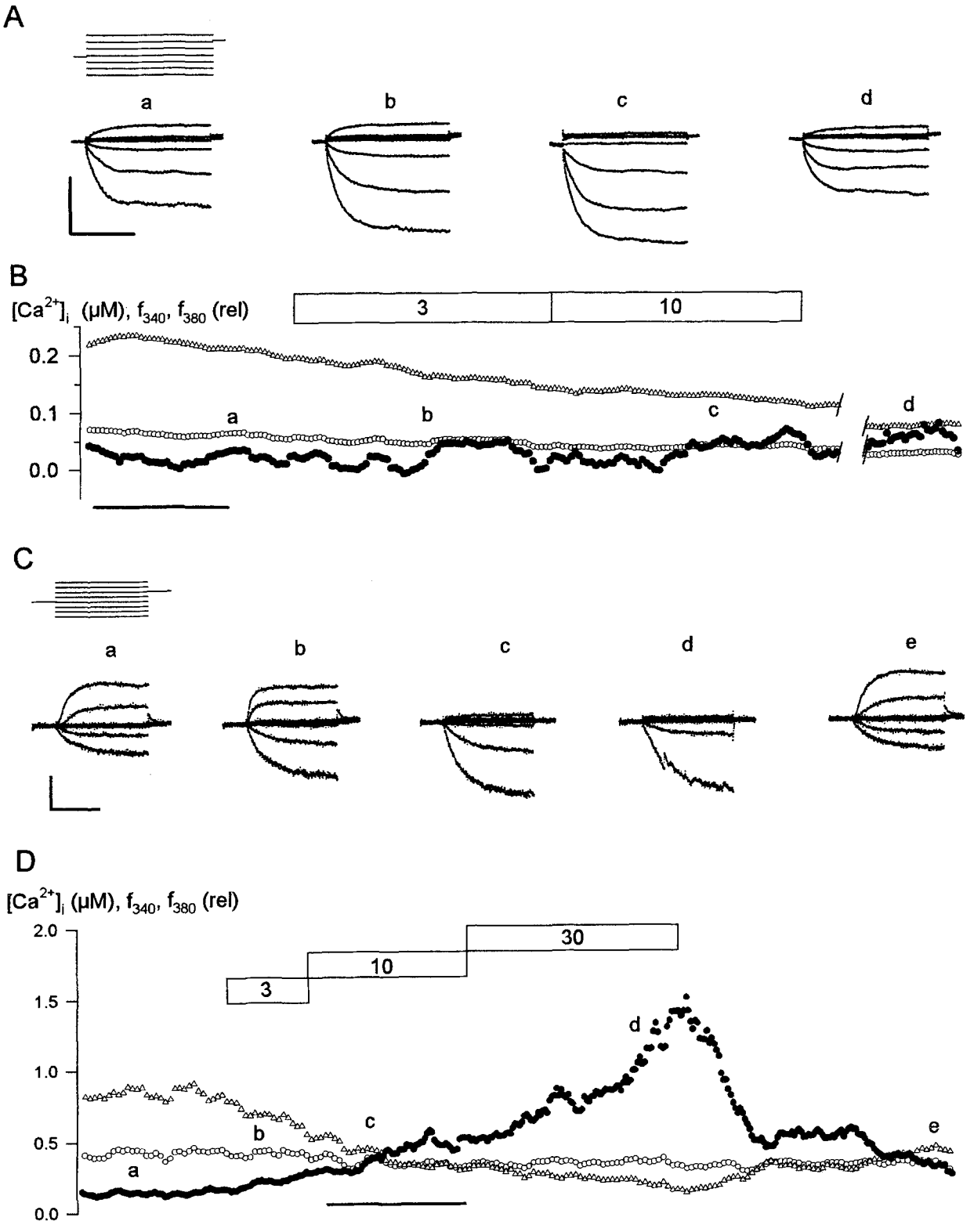

Fig. 7A–D. Rise in cytosolic-free $[Ca^{2+}]$ ($[Ca^{2+}]_i$) accompanies extreme acid pH_i loads in approximately half of measurements from *Vicia* guard cells. Representative data from two cells (**A+B** and **C+D**) bathed in 5 mM Ca^{2+}-Mes (pH 6.1) with 10 mM KCl and with additions of 3, 10 and 30 mM Na^+-butyrate as indicated. Cell parameters: **A+B** surface area, $3.6 \cdot 10^{-5}$ cm^2; volume, 4.7 pl; aperture, 8 μm; **C+D** surface area, $4.1 \cdot 10^{-5}$ cm^2; volume, 5.0 pl; aperture, 10 μm. **A**, **C** Voltage-clamp cycles (*top left*) and current traces recorded at times cross-referenced to the pH_i record in **B** and **D** by letter (*a,b,...e*). Voltage cycles: conditioning voltage, −100 mV; test voltages, 0 to −190 mV (**A**) and +40 to −210 mV (**C**); tailing voltage, −30 mV. Scales: **A** vertical, 250 mV or 100 μA · cm^{-2}; · horizontal, 1 s; **C** vertical, 250 mV or 20 μA · cm^{-2}; horizontal, 1 s. (**B, D**) Time course of experiments with Fura-2 fluorescence recordings (*left scale*) with excitation at 340 (f_{340}, ○) and 380 nm (f_{380}, △) fluorescence signals (*below*) and their ratio (●, calibrated for $[Ca^{2+}]_i$). Time scale (*below*), 2 min. Time bars (*above*) indicate periods of exposures to Na^+-butyrate. Letters (*a,b,c,...e*) indicate times of voltage-clamp scans

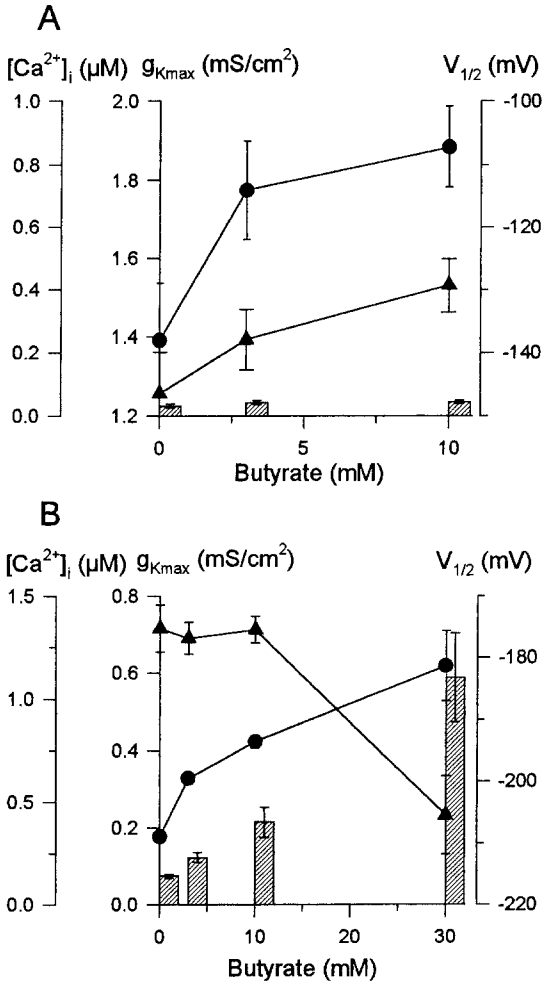

Fig. 8A,B. Acid pH_i-induced rise in cytosolic-free $[Ca^{2+}]$ ($[Ca^{2+}]_i$) displaces the voltage-dependence of $I_{K,in}$ gating negative. Analysis of data from Fig. 7A,B (**A**) and Fig. 7C,D (**B**). Conductance maxima ($g_{K,max}$, ●) and voltages ($V_{1/2}$, ▲) giving half-maximal conductance determined as in Fig. 3 and shown ± SD of the fitted parameter; $[Ca^{2+}]_i$ (*shaded bars*) given as means ± SE of measurements during the period of the corresponding voltage-clamp scan. Note the pronounced negative shift in $V_{1/2}$ with the rise in $[Ca^{2+}]_i$ from approx. 400 nM to near 1 μM

and the ratio of the respective fluorescence emissions f_{340}/f_{380} (= $R_{340/380}$) was used to quantify $[Ca^{2+}]_i$.

The results from two guard cells, shown in Fig. 7, are typical of these recordings. The fluorescence ratio and current traces from one cell in the first two panels showed a $[Ca^{2+}]_i$ signal around 80–100 nM that was virtually unaffected by exposures to Na^+-butyrate (Fig. 7B), and both K^+ channels responded in characteristic fashion with acid-going pH_i. Exposure to 10 mM Na^+-butyrate – which was expected to "clamp" pH_i near 7.0 (see Figs. 1 and 2) – increased the amplitude of $I_{K,in}$ by approximately 60%, inactivated $I_{K,out}$, and both currents recovered on washing the Na^+-butyrate from the bath (Fig. 7A). By contrast, in the second guard cell $[Ca^{2+}]_i$ increased significantly on exposure to 10 mM Na^+-butyrate, and exceeded 1 μM $[Ca^{2+}]_i$ when the acid load was further increased, before recovering after Na^+-butyrate washout (Fig. 7D). Again, the acid loads effectively reduced $I_{K,out}$ and increased $I_{K,in}$ amplitudes. Note that $I_{K,in}$ response in this case was biased to negative voltages: $I_{K,in}$ was reduced at clamp steps to −185 mV relative to steps to −240 mV (compare lowermost traces in Fig. 7C, a–e) when Na^+-butyrate was raised especially to 30 mM outside.

A detailed analysis of these records is shown in Fig. 8 and compares the effects of the acid loads with changes in $[Ca^{2+}]_i$ and the $I_{K,in}$ parameters $g_{K,max}$ and $V_{1/2}$. The K^+ currents were subjected to joint fittings to Eq. 1, with δ and E_K held in common as in Fig. 3, and the $[Ca^{2+}]_i$ signals were averaged over the time periods of the voltage-clamp scans at each Na^+-butyrate concentration. Figure 8A shows that, in the absence of a measurable change in $[Ca^{2+}]_i$, acid pH_i primarily affected $g_{K,max}$. A small shift in $V_{1/2}$ was determined in this case, but the effect of acid-going pH_i was to displace $V_{1/2}$ positive and was not very significant, even in 10 mM Na^+-butyrate. In the second guard cell, $g_{K,max}$ also increased in parallel with the acid pH_i load but, as $[Ca^{2+}]_i$ rose significantly above the resting level, $V_{1/2}$ was driven negative by 33 mV in 30 mM Na^+-butyrate.

Comparable recordings were obtained from a total of 11 experiments with the Fura-2-loaded cells. The recordings divided almost equally between two pools, although no apparent difference could be identified from the controls, which yielded a mean resting $[Ca^{2+}]_i$ of 118 ± 38 nM. In only six cells was a significant change in $[Ca^{2+}]_i$ observed in the presence of acid pH_i loads, and then only in 10 and 30 mM Na^+-butyrate. Furthermore, in every case that lowering pH_i evoked an increase in $[Ca^{2+}]_i$, the effect of pH_i on $I_{K,in}$ was biased to voltages negative of −200 mV, and the $I_{K,in}$ activation effected by the acid pH_i load was reduced at more-positive voltages. These observations pointed to distinct actions of pH_i and $[Ca^{2+}]_i$ on the K^+ channels, but also indicated that measurements of $I_{K,in}$, especially at pH_i values below 7.0, were prone to underestimate the true effect of pH_i on the K^+ current. We return to these points below.

Discussion

The action of cytoplasmic pH in modulating the activity of the K^+ inward-rectifier argues strongly for a dual pattern of ionic second-messenger control as well as demonstrating an interaction between $[Ca^{2+}]_i$ and pH_i in *Vicia* guard cells. Four key lines of evidence support a role for pH_i in controlling $I_{K,in}$ independent of $[Ca^{2+}]_i$. (i) Cytosolic pH had a profound influence on $I_{K,in}$, increasing the current by as much as fivefold with decreasing pH_i from 7.6 to 7.0 (Figs. 1, 3, 6; Table 1). This action was complete within the timescale of the pH_i changes and was fully reversible on washing the weak acid from the bath. (ii) The influence of pH_i on $I_{K,in}$ was independent of membrane voltage (Figs. 3, 4, 5). (iii) Activation of the K^+ current was a simple function of pH_i, consistent with the titration of a single H^+-binding site with a pK_a near 6.4 (Fig. 6; Table 1). (iv) Finally, cytosolic acidification from resting pH_i to 7.1–7.3, which evoked an appreciable stimulation of $I_{K,in}$, was com-

monly achieved without significant change in $[Ca^{2+}]_i$. Even when affected, the response was invariably to increase $[Ca^{2+}]_i$ and to displace the voltage-dependence of gating, characterised by $V_{1/2}$, negative (Figs. 7, 8).

An analysis of acid loads imposed with Na^+-butyrate and Na^+-acetate yielded virtually identical values for cytoplasmic buffer capacities and indicated an apparent buffer content of 275 mM with a pK_a of 6.9 (Fig. 2). These results discount any specific or metabolic interference from the acid anion. So, the first three points implicate a discrete H^+-binding site, in close proximity to the K^+ channels, that acts as a pH_i sensor. They also distinguish $I_{K,in}$ in the guard cells from other Ca^{2+}-dependent K^+ channels, including, maxi-K^+ channels of animal epithelia and inward-rectifiers of ascidian eggs (Moody and Hagiwara 1982; Klaerke et al. 1993) that normally inactivate at acid pH_i. The final point separates the pH_i signal and its control of $I_{K,in}$ from effects mediated through parallel $[Ca^{2+}]_i$-dependent signal processing.

Cytosolic pH and $[Ca^{2+}]_i$ act independently in controlling the K^+ channels. Control of current through the inward-rectifying K^+ channels has generally been linked to Ca^{2+}. Elevating $[Ca^{2+}]_i$ to micromolar concentrations is known to displace the voltage dependence of $I_{K,in}$ negative, and thus to reduce its amplitude at any one voltage (Lemtiri-Chlieh and MacRobbie 1994; Schroeder and Hagiwara 1989), although the precise mechanism of $[Ca^{2+}]_i$ action remains unresolved. Equally, a growing body of evidence has indicated that $I_{K,in}$, or of one of the major signalling elements controlling these channels, is sensitive to pH_i. Lowering pH_i through application of weak acids was found to activate $I_{K,in}$ (Blatt 1992; Blatt and Armstrong 1993), and the current was suppressed during experimentally imposed alkaline pH_i loads (Blatt and Armstrong 1993). Furthermore, molecular genetic studies have indicated the ABI1 gene product – a PP-2C protein phosphatase – also contributes to the regulation of $I_{K,in}$ in the presence of ABA, plausibly by modulating the sensitivity of the channels to pH_i, but independent of $[Ca^{2+}]_i$ (Armstrong et al. 1995). Nonetheless, separating $[Ca^{2+}]_i$- and pH_i-dependent actions on $I_{K,in}$ has been complicated as much by an uncertainty in quantifying the associated characteristics of $I_{K,in}$ as by a lack of information about the changes in $[Ca^{2+}]_i$ effected by pH_i transients.

In terms of current amplitude alone, a simple, opposing action of Ca^{2+} (Schroeder and Hagiwara 1989; Blatt et al. 1990; Lemtiri-Chlieh and MacRobbie 1994) and H^+ (see Figs. 1, 3, 7) on $I_{K,in}$ would not distinguish between the possibilities (i) of separate actions of the two ions or (ii) of their competition for a common binding site in controlling the K^+ channels. However, we found that altering pH_i was without appreciable effect on the voltage-dependence for channel gating ($V_{1/2}$, see Fig. 4) or $I_{K,in}$ relaxation kinetics (Fig. 5), even when the effective cytosolic-free $[H^+]_i$ was varied over more than fivefold. By contrast, increasing $[Ca^{2+}]_i$ was associated with pronounced negative displacements of $V_{1/2}$ and was also seen to slow $I_{K,in}$ activation (Figs. 7, 8; see also Schroeder and Hagiwara 1989; Blatt et al. 1990; Lemtiri-Chlieh and MacRobbie 1994). Such kinetically unique actions on $I_{K,in}$ argue strongly in favour of two discrete control processes that converge independently on the channels. Simple competition of Ca^{2+} and H^+ for a common binding site, whether on the channel protein itself or on an associated protein, would be expected to show opposing actions on the current kinetics and voltage-dependence *as well as* on $I_{K,in}$ amplitude. The same conclusion must be reached for any proposal in which pH_i action is mediated simply through a change in Ca^{2+} binding affinity, including proposals in which H^+ and Ca^{2+} bind at different sites and interact allosterically (Cook et al. 1984; Laurido et al. 1991; Klaerke et al. 1993). Instead, these are fundamental differences that are most easily reconciled with Ca^{2+} and H^+ action at physically discrete sites that ultimately lead to distinct channel protein conformations. This interpretation is broadly consistent also with previous evidence for a redundancy of controls acting on $I_{K,in}$, notably the possibility that K^+ channel and stomatal response to ABA may proceed in the absence of an appreciable change in $[Ca^{2+}]_i$ (Blatt and Armstrong 1993; Allan et al. 1994; Armstrong et al. 1995; Blatt and Grabov 1996). The explanation does not rule out additional competitive effects of H^+ with Ca^{2+} action on the K^+ channels. Positive shifts of $V_{1/2}$ at pH_i values near and below 7.0 (Fig. 3, 8), especially, might be understood in the context of Ca^{2+} displacement from regulatory sites associated with the channels. The action of $[Ca^{2+}]_i$ on $V_{1/2}$ may also point to a cooperative interaction of the divalent with the channels (Fig. 8) analogous to its action on Ca^{2+}-activated K^+ channels of skeletal muscle (Christensen and Zeuthen 1987; Laurido et al. 1991), and this relationship will now require closer scrutiny.

Cytosolic pH gates K^+-channel activity. How does pH_i effect an activation of the K^+ channels from the cytosolic face of the membrane? One possible mechanism could entail a direct interaction of H^+ at a site within the channel pore. Nonetheless, it is difficult to conceive of $I_{K,in}$ activation arising from H^+ interaction at such a site, at least in the conventional sense. Competition between the H^+ and K^+ for a common binding site in the permeation pathway would be expected to effect a reduction in the K^+ current. The action in this case might be through a "flickery" block and apparent reduction in single-channel conductance (Prod'hom et al. 1987) or through an effect on channel open probability and consequent displacement of the voltage-dependence of gating (Cook et al. 1984; Laurido et al. 1991; Klaerke et al. 1993).

Instead, the current characteristics are most easily reconciled with an effect of pH_i mediated through allosteric interactions that result in an increase in the pool of active channels, or possibly in the single-channel conductance. This interpretation is consistent with the insensitivity of $V_{1/2}$ and current activation kinetics to pH_i (Figs. 4, 5), and with the scalar increase in the current (Fig. 3). In this respect, $I_{K,in}$ behaviour parallels

that reported for the K^+ outward-rectifiers of guard cells (Blatt and Armstrong 1993; and Figs. 5 and 7, this paper) and yeast (Lesage et al. 1996), although in these instances lowering pH_i appears to reduce the pool of functional channels. It is worth noting that the voltage-independence of H^+ action inside contrasts with the effect of extracellular H^+ on the current. Like its response to lowered pH_i, increasing $[H^+]$ outside promotes the K^+ current, but in a voltage-dependent manner shifting $V_{1/2}$ positive-going by roughly 22 mV/$[H^+]$ decade and accelerating $I_{K,in}$ activation kinetics (Blatt 1992). The contrast and, in this instance, the sidedness of H^+ action indicate that H^+ must interact with the inward-rectifying K^+ channels at two distinct sites and with differing mechanisms.

At a biochemical level, the present data offer fewer clues about $[H^+]_i$ interaction with the K^+ channels. The apparent pK_a for $I_{K,in}$ activation, near 6.3 (Fig. 6; Table 1) is somewhat lower than might be anticipated for the titration of a critical histidine residue (pK_a = 6.5 in free solution). However, this estimate was particularly sensitive to measurements at the acid pH_i extreme and would be displaced to a lower (more acid) value if $I_{K,in}$ were depressed by other factors independent of pH_i. Parallel measurements of $[Ca^{2+}]_i$ indicated that the estimated pK_a – and the subunitary Hill coefficient – probably was subject to interference from $[Ca^{2+}]_i$ at the acid pH_i extreme (see Figs. 6–8). Whether the H^+-binding site is located on the channel protein itself or an associated, regulatory protein is an open question.

Cytosolic pH and $[Ca^{2+}]_i$ interact. Although pH_i- and $[Ca^{2+}]_i$-mediated controls on $I_{K,in}$ are fundamentally distinct, the data in Figs. 7 and 8 nonetheless underscore an interaction between the two signal intermediates upstream of their action on the K^+ channels. Acidifying pH_i, especially to values below about 7.0, frequently was followed by a rise in $[Ca^{2+}]_i$ that increased with the acid load. Even so, these events did not correlate well with the timecourse of solution exchange during butyrate additions (Fig. 7) and, hence, of the pH_i changes imposed. So we are confident in ruling out passive interactions between Ca^{2+} and H^+ entailing bulk titration of fixed charges within cytosolic Ca^{2+}-binding domains and cation exchange (Busa 1986). Instead the scope and variability, both in timecourse and magnitude, of these $[Ca^{2+}]_i$ transients are consonant with an ability of acid pH_i to sensitise the guard cells to other signalling elements, thus indirectly triggering a rise in $[Ca^{2+}]_i$.

At present, the mechanism(s) of this interaction remains unclear. It is very likely that pH_i changes of this magnitude could dramatically alter receptor affinities for ligands, including inositol-1,4,5-trisphosphate and cyclic ADP-ribose (Clapham 1995). Taylor and Richardson (1991) point out that the binding of inositol-1,4,5-trisphosphate to its receptor, as well as the size of internal Ca^{2+} stores in aortic endothelial cells, can show a marked pH_i sensitivity. However, alkaline, rather than acid pH_i favours inositol-1,4,5-trisphosphate-mediated Ca^{2+} release both in animals (Danthuluri et al. 1990) and in plants (Scanlon et al. 1996). Another proven pathway for Ca^{2+} release, the activity of vacuolar SV-type ion channels is also severely impaired in guard cells when pH_i falls below 7.0–7.2 (Schulzlessdorf and Hedrich 1995). Thus, it remains to be seen now whether the observations are related to Ca^{2+} flux across the tonoplast, another organelle membrane or the plasma membrane, and whether they may be linked to pH_i interactions with other cytoplasmic ligands.

We are grateful to M.D. Fricker (Plant Sciences, Oxford) for helpful suggestions in the early stages of this work, and for his and G. Thiel's (Göttingen) critical reading of the manuscript. This work was possible with the aid of grants from the Gatsby Charitable Foundation, the Royal Society the University of London Central Research Fund and the Human Frontiers Science Program. A.G. is supported by grant 32/C098-1 from the Biotechnology and Biological Sciences Research Council.

References

Allan AC, Fricker MD, Ward JL, Beale MH, Trewavas AJ. (1994) Two transduction pathways mediate rapid effects of abscisic acid in *Commelina* guard cells. Plant Cell 6: 1319–1328

Armstrong F, Leung J, Grabov A, Brearley J, Giraudat J, Blatt MR. (1995) Sensitivity to abscisic acid of guard cell K^+ channels is suppressed by *abi1-1*, a mutant *Arabidopsis* gene encoding a putative protein phosphatase. Proc Natl Acad Sci USA 92: 9520–9524

Assmann SM (1993) Signal transduction in guard cells. Annu Rev Cell Biol. 9: 345–375

Blatt MR (1992) K^+ channels of stomatal guard cells: characteristics of the inward rectifier and its control by pH. J Gen Physiol 99: 615–644

Blatt MR, Armstrong F. (1993) K^+ channels of stomatal guard cells: abscisic acid-evoked control of the outward rectifier mediated by cytoplasmic pH. Planta 191: 330–341

Blatt MR, Grabov A. (1996) Signal redundancy, gates and integration in the control of ion channels for stomatal movement. J Exp Bot, in press

Blatt MR, Slayman CL (1983) KCl leakage from microelectrodes and its impact on the membrane parameters of a nonexcitable cell. J Membr Biol 72: 223–234

Blatt MR, Thiel G. (1993) Hormonal control of ion channel gating. Annu Rev Plant Physiol Mol Biol 44: 543–567

Blatt MR, Thiel G, Trentham DR (1990) Reversible inactivation of K^+ channels of *Vicia* stomatal guard cells following the photolysis of caged inositol 1,4,5-trisphosphate. Nature 346: 766–769

Boron WF (1977) Intracellular pH transients in giant barnacle muscle fibers. Am J Physiol 233: 61–73

Busa WB (1986) Mechanisms and consequences of pH-mediated cell regulation. Annu Rev Physiol 48: 389–402

Bush DS, Jones RL. (1990) Measuring intracellular Ca^{2+} levels in plant cells using the fluorescent probes Indo-1 and Fura-2. Plant Physiol 93: 841–845

Christensen O, Zeuthen T (1987) Maxi K^+ channels in leaky epithelia are regulated by intracellular Ca^{2+}, pH and membrane potential. Pfluegers Archiv, Eur J Physiol 408: 249–259

Clapham DE (1995) Calcium signaling. Cell 80: 259–268

Cook DL, Ikeuchi M, Fujimoto WY (1984) Lowering of pH_i inhibits Ca^{2+}-activated K^+ channels in pancreatic B-cells. Nature 311: 269–271

Danthuluri NR, Kim D, Brock TA (1990) Intracellular alkalinization leads to Ca^{2+} mobilization from agonist-sensitive pools in bovine aortic endothelial cells. J Biol Chem 265: 19071–19076

Fairley-Grenot KA, Assmann SM (1992) Permeation of Ca^{2+} through K^+ channels in the plasma membrane of *Vicia faba* guard cells. J Membr Biol 128: 103–113

Fricker MD, Gilroy S, Read ND, Trewavas AJ (1991) Visualisation and measurement of the calcium message in guard cells. In: Schuch W, Jenkins G, (eds.) Molecular biology of plant development. Cambridge Univ. Press, Cambridge, pp 177–190

Gilroy S, Read ND, Trewavas AJ (1990) Elevation of cytoplasmic calcium by caged calcium or caged inositol trisphosphate initiates stomatal closure. Nature 346: 769–771

Gilroy S, Fricker MD, Read ND, Trewavas AJ. (1991) Role of calcium in signal transduction of *Commelina* guard cells. Plant Cell 3: 333–344

Hedrich R, Busch H, Raschke K (1990) Ca^{2+} and nucleotide dependent regulation of voltage dependent anion channels in the plasma membrane of guard cells. EMBO J 9: 3889–3892

Irving HR, Gehring CA, Parish RW (1992) Changes in cytosolic pH and calcium of guard cells precede stomatal movements. Proc Natl Acad Sci USA 89: 1790–1794

Klaerke DA, Wiener H, Zeuthen T, Jorgensen PL (1993) Ca^{2+} activation and pH dependence of a maxi K^+ channel from rabbit distal colon epithelium. J Membr Biol 136: 9–21

Laurido C, Candia S, Wolff D, Latorre R (1991) Proton modulation of Ca^{2+}-activated K^+ channel from rat skeletal muscle incorporated into planar bilayers. J Gen Physiol 98: 1025–1043

Lemtiri-Chlieh F, MacRobbie EAC (1994) Role of calcium in the modulation of *Vicia* guard cell potassium channels by abscisic acid: a patch-clamp study. J Membr Biol 137: 99–107

Lesage F, Guillemare E, Fink M, Duprat F, Lazdunski M, Romey G, Barhanin J (1996) A pH-sensitive yeast outward rectifier K^+ channel with 2 pore domains and novel gating properties. J Biol Chem 271: 4183–4187

Leung J, Bouvier-Durand M, Morris P-C, Guerrier D, Chefdor F, Giraudat J (1994) *Arabidopsis* ABA response gene *ABI1*: features of a calcium-modulated protein phosphatase. Science 264: 1448–1452

MacRobbie EAC (1992) Calcium and ABA-induced stomatal closure. Proc R Soc London B Ser 338: 5–18

Marquardt D (1963) An algorithm for least-squares estimation of nonlinear parameters. J Soc Ind Appl Math 11: 431–441

McAinsh MR, Brownlee C, Hetherington AM (1990) Abscisic acid-induced elevation of guard cell cytosolic Ca^{2+} precedes stomatal closure. Nature 343: 186–188

McCormack JG, Cobbold PH (1991) Cellular calcium, vol 1. Oxford University, Oxford

Meyer K, Leube MP, Grill E. (1994) A protein phosphatase 2C involved in ABA signal transduction in *Arabidopsis thaliana*. Science 264: 1452–1455

Moody WJ, Hagiwara S (1982) Block of inward rectification by intracellular H^+ in immature oocytes of the starfish *Mediaster aequalis*. J Gen Physiol 79: 115–130

Morris SJ, Wiegmann TB, Welling LW, Chronwall BM (1994) Rapid simultaneous estimation of intracellular calcium and pH. In: Nuccitelli RQ (ed) A practical guide to the study of calcium in living cells. Academic Press, London, pp 183–220

Prod'hom B, Pietrobon D, Hess P (1987) Direct measurement of proton transfer rates to a group controlling the dihydropyridine-sensitive Ca^{2+} channel. Nature 329: 243–246

Purves JD (1981) Microelectrode methods for intracellular recording and ionophoresis. Academic Press, London, pp 1–146

Roos A, Boron WF (1981) Intracellular pH. Physiol Rev 61: 296–434

Scanlon CH, Martinec J, Machackova I, Rolph CE, Lumsden PJ (1996) Identification and preliminary characterization of a Ca^{2+}-dependent high-affinity binding site for inositol-1,4,5-trisphosphate from *Chenopodium rubrum*. Plant Physiol 110: 867–874

Schroeder JI (1992) Plasma membrane ion channel regulation during abscisic acid-induced closing of stomata. Philos Trans R Soc London B Ser 338: 83–89

Schroeder JI, Hagiwara S (1989) Cytosolic calcium regulates ion channels in the plasma membrane of *Vicia faba* guard cells. Nature 338: 427–430

Schroeder JI, Hagiwara S (1990) Repetitive increases in cytosolic Ca^{2+} of guard cells by abscisic acid: activation of nonselective Ca^{2+} permeable channels. Proc Natl Acad Sci USA 87: 9305–9309

Schroeder JI, Keller BU (1992) Two types of anion channel currents in guard cells with distinct voltage regulation. Proc Natl Acad Sci USA 89: 5025–5029

Schulzlessdorf B, Hedrich R (1995) Protons and calcium modulate SV-type channels in the vacuolar lysosomal compartment-channel interaction with calmodulin inhibitors. Planta 197: 655–671

Segel IH (1993) Enzyme kinetics. Wiley Interscience, New York

Taylor CW, Richardson A (1991) Structure and function of inositol trisphosphate receptors. PharmTher 51: 97–137

Thiel G, Blatt MR, Fricker MD, White IR, Millner PA (1993) Modulation of K^+ channels in *Vicia* stomatal guard cells by peptide homologs to the auxin-binding protein C-terminus. Proc Natl Acad Sci USA 90: 11493–11497

Ward JM, Schroeder JI (1994) Calcium-activated K^+ channels and calcium-induced calcium release by slow vacuolar ion channels in guard-cell vacuoles implicated in the control of stomatal closure. Plant Cell 6: 669–683